

Origin of the formation of the tetragonal phase near the surface of quenched $\text{YBa}_2\text{Cu}_3\text{O}_x$

Shoichi Edo

Department of Mechanical System Technology, Hokkaido Polytechnic College, Zenibako 3-190, Otaru 047-02, Japan

Toshihiko Takama

Department of Applied Physics, Faculty of Engineering, Hokkaido University, Kita-ku, Sapporo 060, Japan

(Received 29 November 1993; revised manuscript received 24 February 1994)

The distribution of structural phases formed in polycrystalline $\text{YBa}_2\text{Cu}_3\text{O}_x$ by quenching has been measured by means of x-ray diffraction. Disk-shaped samples were annealed in a temperature range of 680–800°C in air, and subsequently quenched in liquid nitrogen. The x-ray diffraction patterns revealed that the tetragonal phase is formed near the surface although the orthorhombic phase is distributed entirely in the inside. The depth to the phase boundary increased with increasing sample thickness and annealing temperature. The conclusion is that the tetragonal phase is not a preserved phase from high temperature but a newly produced phase by deoxidation during quenching. The lower concentration of oxygen near the surface was directly confirmed by x-ray photoelectron spectroscopy. It was also confirmed that the transition from superconductor to normal conductor takes place in the orthorhombic phase.

I. INTRODUCTION

The study of the relationship between the crystal structure and the superconductivity in high- T_c superconductors is fundamental in order to clarify the superconducting mechanism. A number of studies concerning the relationship in $\text{YBa}_2\text{Cu}_3\text{O}_x$ have been reported.^{1–9} It is well known that the superconducting transition temperature decreases, showing two plateaus at ~ 90 and at ~ 60 K, and the structure changes from orthorhombic to tetragonal, as oxygen concentration decreases. However, the structural phase in which the change from superconductor to normal conductor takes place has varied depending on the investigator.^{1,4,7–9}

The oxygen concentration has been controlled by annealing temperature and quenching medium in the sample preparation. In regard to quenching, liquid N_2 ,^{1,3,6,9} cooled He gas,⁷ and air^{4,5} have been utilized for the quenching medium. A tetragonal phase has often been observed near the as-quenched surface at room temperature. It has been considered that the tetragonal phase is simply the frozen-in high-temperature phase. To our knowledge, no one has assessed the impact the quenching rate would have on the formation of the phase. We will show that the tetragonal phase is not a preserved phenomenon but is caused by deoxidation during the quenching.

II. EXPERIMENTAL

$\text{YBa}_2\text{Cu}_3\text{O}_x$ was prepared by firing a mixture of powders with the proportions of 3 mol of CuO to 2 mol of BaCO_3 to $\frac{1}{2}$ mol of Y_2O_3 for 24 h at 930°C in air. Reground powders were pressed into disk-shaped pellets at an applied pressure of ~ 300 MPa. Then the pellets were sintered for 24 h at 940°C in air and slowly cooled to room temperature at the rate of 1 K/min. The hydrogen

reduction method resulted in an estimate of oxygen concentration $x = 6.95$. The samples obtained consisted of fine grains with the average size of $10 \times 10 \times 30 \mu\text{m}^3$. The samples were porous and had a density of about 5.4 g/cm^3 which is about 85% of that for a single crystal. The x-ray and resistivity measurements showed that the samples have a single orthorhombic phase at room temperature and a superconducting transition temperature T_c of 90 K. The sintered pellets were thinned to 0.2, 0.6, and 2.0 mm by polishing the surfaces with fine emery papers. Each sample was annealed finally at various temperatures ranging from 680 ($x = 6.48$) to 800°C ($x = 6.28$) for 6 h in air, then quenched into liquid nitrogen. The concentration was obtained from the weight loss measured by thermogravimetry on heating in air.

The structural phases near the surface were determined by taking x-ray diffraction patterns using $\text{Cu } K\alpha$ radiation. After taking the patterns, the surface was removed by a desired thickness using fine emery papers. The phase distribution in the sample was determined by repeating the same measurement and treatment. T_c was obtained by measuring the temperature dependence of dc resistivity for the as-quenched sample using a four probe method. The variation of the oxygen concentration with depth was examined by x-ray photoelectron spectroscopy (XPS).

III. RESULTS

Figure 1 demonstrates a typical example of variation in x-ray diffraction patterns around $2\theta = 58^\circ$ for the 2-mm-thick sample quenched from 760°C ($x = 6.35$). It is seen that the as-quenched surface provides only the diffraction pattern expected from the tetragonal phase. As the surface is removed, the pattern turns to that of the orthorhombic phase.

Figure 2 shows the variations of the lattice parameters

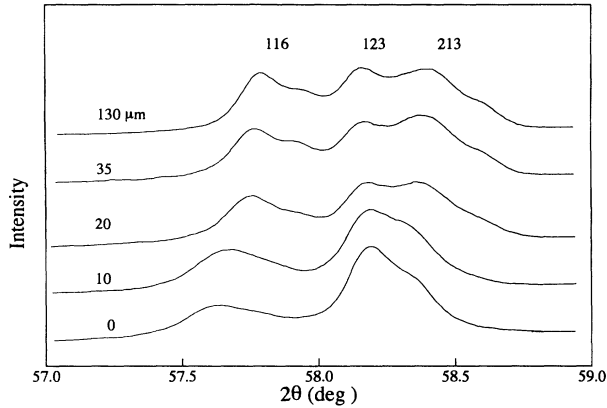


FIG. 1. Variation of x-ray diffraction patterns from the as-quenched surface. Removed thicknesses are 0, 10, 20, 35, and 130 μm from the bottom. Peaks correspond to the 116, 123, and 213 reflections for the orthorhombic structure.

a , b , and $c/3$ obtained from the sample for Fig. 1 as a function of depth. The three parameters remain at constant values at the deeper positions (more than 50 μm). It is noted that the phase varies at the depth between 5 and 10 μm as seen from the lattice parameters a and b . X-rays penetrate into the sample to some extent. The mass absorption coefficient of 171 cm^2/g for Cu $K\alpha$ radiation¹⁰ and the sample density of 5.4 g/cm^3 yield the linear absorption coefficient of 930 cm^{-1} for the present experiment. For the Bragg angle of 20°, about 90% of the measured x rays are obtained from the surface layer between 0 and 6 μm . Hence the depth does not correspond to the exact distance from the as-quenched surface.

Figure 3 displays the depth (D_{10}) of the phase bound-

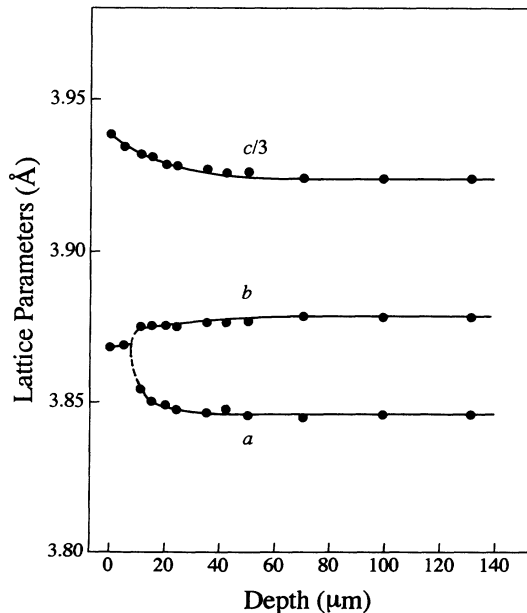


FIG. 2. Variation of lattice parameters as a function of depth. The sample has a thickness of 2 mm and is quenched from 760°C. A phase boundary is seen between 5 and 10 μm in depth.

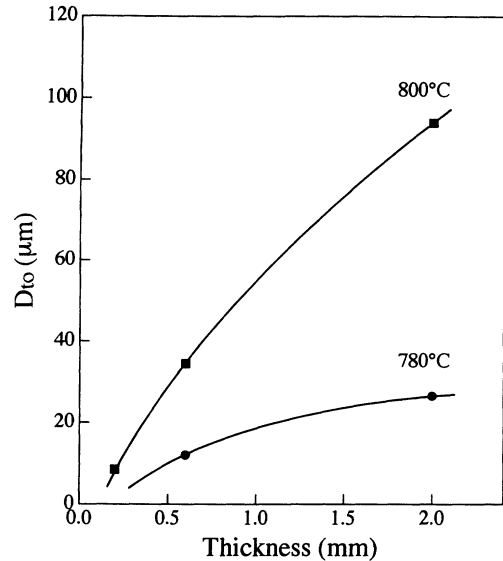


FIG. 3. Depth D_{10} to phase boundary versus sample thickness for the samples quenched from 780° and 800°C. The upper and the lower regions of each line correspond to orthorhombic and tetragonal phases, respectively.

ary between tetragonal and orthorhombic structures for the samples quenched from 780 ($x=6.31$) and 800°C ($x=6.28$) as a function of sample thickness. D_{10} increases with an increase in initial thickness of sample as well as with an increase in annealing temperature. The sample with 0.2 mm thickness quenched from 780°C showed only the orthorhombic phase. For the 2-mm-thick sample quenched from 800°C, D_{10} reached 90 μm . D_{10} for the samples quenched from 780°C is smaller than that from 800°C for the sample thickness. From these ob-

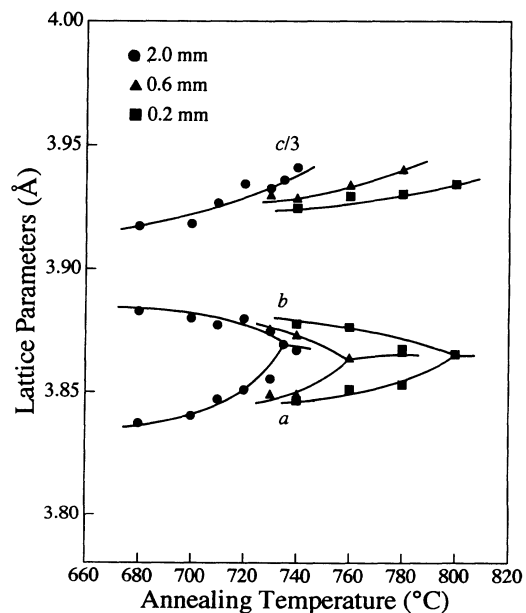


FIG. 4. Change of lattice parameters a , b , and $c/3$ due to annealing temperature measured for as-quenched surfaces of 0.2-, 0.6-, and 2.0-mm-thick samples.

servations, one sees that D_{10} is sensitive to sample thickness and annealing temperature.

The lattice parameters measured for the as-quenched surfaces are shown in Fig. 4 as a function of annealing temperature. The annealing temperature at which the structure changes from orthorhombic to tetragonal is 735°C for the 2-mm-thick sample, 760°C for 0.6 mm, and 800°C for 0.2 mm. The temperature shifts to the low-temperature side with an increase in the sample thickness.

IV. DISCUSSION

It is known that the equilibrium phase of $\text{YBa}_2\text{Cu}_3\text{O}_x$ in air is tetragonal at temperatures greater than about 650°C ($x=6.5$).¹¹⁻¹³ If the tetragonal phase is preserved during quenching, D_{10} should increase with a decrease in sample thickness, because the quenching rate becomes higher as the thickness decreases. The prediction is completely opposite to the present experimental results shown in Fig. 3. The results can be interpreted by considering deoxidation accompanying oxygen diffusion near the surface layer.

The present samples were quenched into liquid nitrogen with oxygen partial pressure of ~ 0 Pa. The equilibrium concentration of oxygen becomes lower with decreasing partial pressure of oxygen.^{14,15} Hence, under the present conditions, the samples should deoxidize until the temperature decreases to a critical level below which no oxygen-atom diffusion occurs. The degree of deoxidation is highest in the surface. This induces the structural transition from the orthorhombic to the tetragonal structure near the surface, as observed. Since the deoxidation period is shorter for thinner samples, the depth D_{10} is expected to decrease with decreasing sample thickness, as seen in Fig. 3. For a thinner sample quenched from a lower temperature, the quenching will be completed before deoxidation. This is thought to be the reason why a tetragonal phase was not observed in the 0.2-mm-thick sample quenched from 780°C. Based on this idea, the shift of the structural transition temperature for the as-quenched sample shown in Fig. 4 can be understood. At greater depth, the lattice parameters are constant, as shown in Fig. 2. This indicates that oxygen concentration is uniform in the inner part. The change in D_{10} for the annealing temperature shown in Fig. 3 reflects that the equilibrium oxygen concentration in the sample is lower at higher annealing temperatures.

The distribution of oxygen concentration is roughly estimated by the diffusion equation¹⁶ assuming that the sample is a continuum. The concentration $x(d,t)$ at depth d and at time t after quenching for a $\text{YBa}_2\text{Cu}_3\text{O}_{6+\delta_0}$ plate with thickness h and infinite area is given by

$$x(d,t) = \frac{4\delta_0}{\pi} \sum_{j=0}^{\infty} \frac{1}{(2j+1)} \sin \frac{(2j+1)\pi d}{h} \times \exp \left[- \left(\frac{(2j+1)\pi}{h} \right)^2 Dt \right] + 6, \quad (1)$$

where D is the diffusion constant. Here the oxygen atoms are assumed to diffuse out until x decreases to 6 in N_2 gas.¹⁷ The concentration $x(d,t)$ was calculated using the measured value of $D = 10^{-5} \text{ cm}^2/\text{sec}$.¹⁸⁻²¹ Examples of concentration profiles that are obtained after different times are shown in Fig. 5. We know no exact value of the cooling rate in liquid nitrogen. Thus, it was assumed that the sample is held at 800°C ($\delta_0=0.28$) for the periods shown in Fig. 5. The figure shows that the tetragonal phase is formed at deeper positions as the holding time increases. When we assume that the transition takes place at $x=6.15$,⁸ the profiles give the calculated D_{10} with 8–42 μm for holding times of 0.1–2 sec. They explain the observed depth.

In the above estimation, continuum matter was assumed for the sample. Here, the effect of porosity in the sample on the diffusion of oxygen is considered. The oxygen atoms might diffuse out in two ways. One is out-diffusion from the surface layer into the nitrogen around the surface and the other is diffusion into the porosity in the sample. When a sample is porous, the contact area with nitrogen increases in comparison with the sample with high density. The outdiffusion takes place more easily and the diffused-out oxygen can be replaced by nitrogen. The replacement lowers the oxygen partial pressure in the surrounding area. This activates the deoxidation on the surface. The grain size of the specimen used, however, has only the dimensions of $10 \times 10 \times 30 \mu\text{m}^3$. Thus, the contact area between grains becomes narrower and interdiffusion between grains will be prevented. This is counteracted by the outdiffusion into porosities in the specimen.²¹ The porosities in the deep positions will be isolated from the outside of the specimen and contain oxygen atoms in equilibrium. This means deoxidation is hard in the deeper positions. On the other hand, the porosities near the surface should be connected to the outside through the porosities between the grains. In this case, the oxygen atoms from the grains can diffuse to the porosities and can be replaced by nitrogen atoms. This

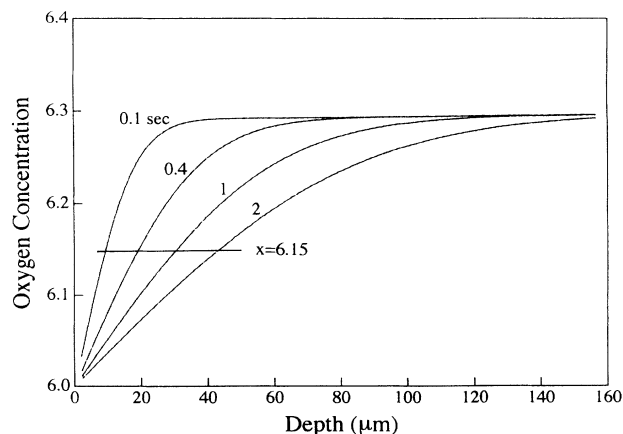


FIG. 5. Calculated profiles of oxygen concentration x for sample quenched from 800°C with thickness of 2 mm. The sample is assumed to be held at 800°C for the periods shown in the figure.

prompts the deoxidation near the surface. The depth deoxidized increases as the cooling rate decreases, that is, sample thickness increases, because the atomic replacement is enhanced. These circumstances are thought to be the reason for formation of the phase distribution near the surface.

The lack of oxygen at the surface was directly confirmed by x-ray photoelectron spectroscopy. Figure 6 shows parts of the XPS signals from the as-quenched surface and from a depth of $130\ \mu\text{m}$, respectively. The peaks at around $933\ \text{eV}$ and the satellite peaks at $943\ \text{eV}$ correspond to signals for $\text{Cu } 2p_{3/2}$ electrons and for the Cu-O bond, respectively. The ratio of the satellite intensity to the main intensity measured for the inside is roughly 1.4 times the ratio for the as-quenched surface. This means that the oxygen concentration in the surface layer is lower than in the inside. No XPS signal for the $\text{N } 1s$ state at around $398\ \text{eV}$ was detected for the quenched surface layer. This fact indicates that no replacement of oxygen atoms by nitrogen atoms takes place in the lattice.

T_c (onset) is shown in Fig. 7 as a function of annealing temperature. T_c for the 0.2-mm-thick sample is higher than that for the 2.0-mm sample. By extrapolating T_c to zero, we can estimate the critical annealing temperature over which no sample shows the superconducting transition. The temperatures are approximately 750°C ($x = 6.36$) and 780°C ($x = 6.31$) for samples with 2.0 and 0.2 mm thicknesses, respectively. The lower T_c for the thicker sample might originate from a slight deoxidation of the whole sample during quenching.

The contribution of the surface layer with the tetragonal phase to superconductivity can be neglected, because the volume fraction of the layer is negligibly small in comparison with that of the internal orthorhombic region. The orthorhombic structure is stable up to the annealing temperature of 800°C ($x = 6.28$) near the surface as shown in Fig. 4. It should be emphasized that the transition from the superconductor to normal conductor takes place only in the orthorhombic phase. From a first

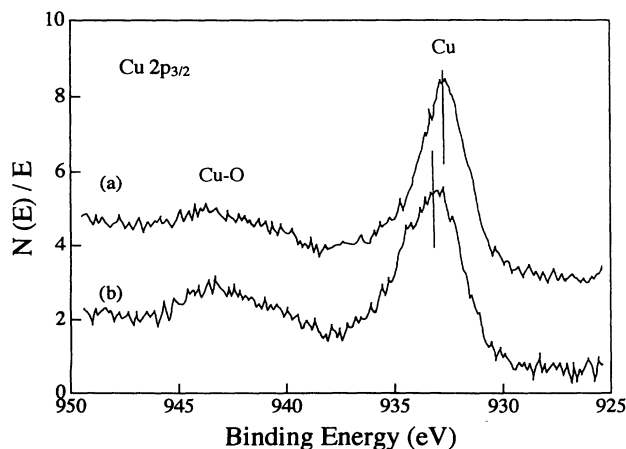


FIG. 6. XPS signals of $\text{Cu } 2p_{3/2}$ and of the Cu-O bond detected for the 2-mm-thick sample quenched from 760°C (a) for the as-quenched surface and (b) for the depth of $130\ \mu\text{m}$.

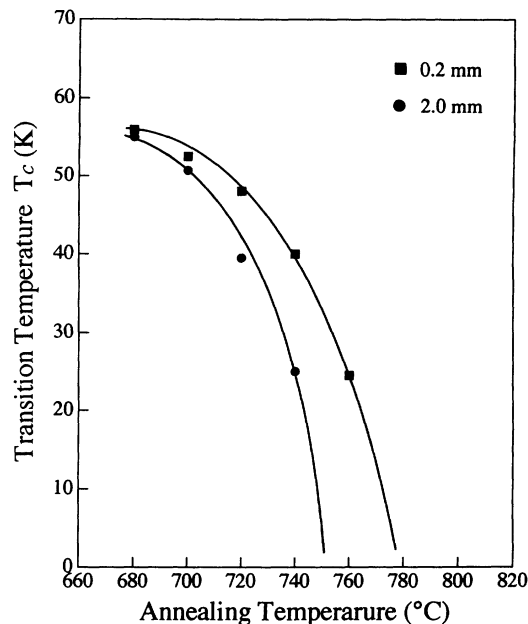


FIG. 7. T_c (onset) versus annealing temperature measured for the 0.2- and 2.0-mm-thick samples.

look at Figs. 4 and 7 for the 2-mm-thick sample, it might seem that the transition happens in the tetragonal phase, but this is not correct. The measured parts are the surface for structural phase and the inside for superconductivity. From the results, the disagreement about the relationship between structure and superconductivity in the studies^{1,4,7,9} so far reported is thought to be caused by the quenching conditions such as quenching medium and sample dimensions.

V. SUMMARY

We have clarified the origin of tetragonal phase formation near the surface of polycrystalline $\text{YBa}_2\text{Cu}_3\text{O}_x$ quenched into liquid nitrogen. A change of phase from tetragonal to orthorhombic was observed near the surface by means of x-ray diffraction. The depth to the phase boundary decreases with a decrease in sample thickness, that is, with an increase in cooling rate. A lower concentration of oxygen near the surface than internally was observed by XPS. The phenomena show that the surface tetragonal phase is formed by deoxidation due to oxygen outdiffusion during the quenching treatment. The present study also concludes that the transition from superconductor to normal conductor takes place in the orthorhombic phase.

ACKNOWLEDGMENTS

The authors wish to acknowledge Thomas W. Little of the University of Washington for his critical reading of this manuscript and Dr. T. Hashizume for his assistance in the XPS measurements.

- ¹E. T. Muromachi, Y. Uchida, M. Ishii, T. Tanaka, and K. Kato, *Jpn. J. Appl. Phys.* **26**, L1156 (1987).
- ²F. Izumi, H. Asano, T. Ishigaki, E. T. Muromachi, Y. Uchida, and N. Watanabe, *Jpn. J. Appl. Phys.* **26**, L1193 (1987).
- ³F. Izumi, H. Asano, T. Ishige, E. T. Muromachi, Y. Uchida, and N. Watanabe, *Jpn. J. Appl. Phys.* **26**, L1214 (1987).
- ⁴R. J. Cava, B. Batlogg, C. H. Chen, E. A. Rietman, S. M. Zahurak, and D. Werder, *Phys. Rev. B* **36**, 5719 (1987).
- ⁵G. V. Tendeloo, H. W. Zandbergen, and S. Amelinckx, *Solid State Commun.* **63**, 603 (1987).
- ⁶S. Nakanishi, M. Kogachi, H. Sasakura, N. Fujioka, S. Minamigawa, K. Nakahigashi, and Akira Yanase, *Jpn. J. Appl. Phys.* **27**, L329 (1988).
- ⁷W. Wong-Ng, L. P. Cook, C. K. Chiang, L. J. Swartzendruber, L. H. Bennett, J. Blendell, and D. Minor, *J. Mater. Res.* **3**, 832 (1988).
- ⁸Y. Ueda and K. Kosuge, *Physica C* **156**, 281 (1988).
- ⁹J. D. Jorgensen, B. W. Veal, A. P. Paulikas, L. J. Nowicki, G. W. Crabtree, H. Claus, and W. K. Kwok, *Phys. Rev. B* **41**, 1863 (1990).
- ¹⁰*International Tables for X-ray Crystallography*, edited by C. H. Macgillavry, G. D. Rieck, and K. Lonsdale (Kynoch, Birmingham, 1962), Vol. III.
- ¹¹J. D. Jorgensen, M. A. Beno, D. G. Hinks, L. Soderholm, K. J. Volin, R. L. Hitterman, J. D. Grace, and I. K. Schuller, *Phys. Rev. B* **36**, 3608 (1987).
- ¹²P. P. Freitas and T. S. Plakett, *Phys. Rev. B* **36**, 5723 (1987).
- ¹³A. T. Fiory, M. Gurvitch, R. J. Cava, and G. P. Espinosa, *Phys. Rev. B* **36**, 7262 (1987).
- ¹⁴K. Kishio, J. Shimoyama, T. Hasegawa, K. Kitazawa, and K. Fueki, *Jpn. J. Appl. Phys.* **26**, L1228 (1987).
- ¹⁵H. M. O'Bryan and P. K. Gallagher, *J. Mater. Res.* **3**, 619 (1988).
- ¹⁶P. G. Shewmon, *Diffusion in Solids* (McGraw-Hill, New York, 1963).
- ¹⁷S-F. Lau, A. B. Rosenthal, N. P. Pyrrros, J. A. Graham, and H. N. Cheng, *J. Mater. Res.* **6**, 227 (1991).
- ¹⁸J. H. Park and P. Kostic, *Mater. Lett.* **6**, 393 (1988).
- ¹⁹K. Kishio, K. Suzuki, T. Hasegawa, T. Yamamoto, and K. Kitazawa, *J. Solid State Chem.* **82**, 192 (1989).
- ²⁰D. Shi, J. Kruczkak, M. Tang, N. Chen, and R. Bhadra, *J. Appl. Phys.* **66**, 4325 (1989).
- ²¹J. R. LaGraff and D. A. Payne, *Phys. Rev. B* **47**, 3380 (1993).